Electronic Supplementary Information

An ESIPT-induced NIR fluorescent probe visualizing mitochondrial sulfur dioxide during oxidative stress in *vivo*

Haixian Ren,[a,c] Fangjun Huo,[b] Xia Wu,[d] Xiaogang Liu, *[d] Caixia Yin*[a]

[a] *Key Laboratory of Chemical Biology and Molecular Engineering of Ministry of Education, Key Laboratory of Materials for Energy Conversion and Storage of Shanxi Province, Institute of Molecular Science, Shanxi University, Taiyuan 030006, China. E-mail: yincx@sxu.edu.cn*

[b] *Research Institute of Applied Chemistry, Shanxi University, Taiyuan 030006, China.*

[c] *Xinzhou Teachers University, Xinzhou 030004, China.*

Singapore University of Technology and Design, 8 Somapah Road, Singapore 487372.

I: Material and Methods

II: Figures

Table S1: The details of the reported probe for sulfite.

Scheme S1: The synthesis compound of **NIR-TS.**

Figure S1: ^{1}H NMR, ^{13}C NMR, and HR-MS spectrum of **NIR-TS**.

Figure S2: Evaluation on the response of **NIR-TS** (30 μM) toward Na_2SO_3.

Figure S3: Dynamic analysis of the response of **NIR-TS** (30 μM) toward Na_2SO_3.

Figure S4: Intensities at 836 nm of probe **NIR-TS** upon addition of different analytes

Figure S5: The HR-MS of the **NIR-TS**-Na_2SO_3 system.

Figure S6: Theoretical chemical calculation about the optical mechanism.

Figure S7: Cell viability estimated by MTT-8 assay with Hela cells.

Figure S8: Imaging experimen about targeting mitochondrial.

Figure S9: Imaging the sulfite in the cells.

Figure S10: Imaging the sulfite in the cells during oxidative stress.

Ⅲ：**References**

I: Material and Methods

Materials. All chemicals and were purchased from commercial suppliers and used without further purification. All solvents were purified prior to use. Distilled water was used after passing through a water ultra-purification stem. TLC analysis was performed using precoated silica plates. Hitachi F−7000 fluorescence spectrophotometer was employed to measure fluorescence spectra. Hitachi U-3900 UV-vis spectrophotometer was employed to measure UV-vis spectra. Shanhai Huamei Experiment Instrument Plants, China provided a PO-120 quartz cuvette (10 mm). ^{1}H NMR and ^{13}C NMR experiments were performed with a BRUKER AVANCE III HD 600 MHz and 151 MHz NMR spectrometer, respectively (Bruker, Billerica, MA). Coupling constants (*J* values) are reported in hertz. HR-MS determinations were carried out on an AB SCIEX TripleTOF 5600 Instruments. The cell imaging experiments were measured by Zeiss LSM880 Airyscan confocal laser scanning microscope. Semiquantitative experiments of cellular fluorescent intensitis were measured by a Tecan infinite 200Pro plate reader.

Synthesis. The synthesis route of probe **NIR-TS** was shown in Scheme S1. Compound **1** (0.71 g, 2 mmol) and Compound **2** (1.08 g, 4 mmol) were dissolved in 30 mL CH_3COOH. The mixture was heated at 110 °C for 2 h. After the reaction was completed, the solvent was removed to give the crude product. Then, dried and subjected to purification by flash chromatography (CH_2Cl_2 : CH_3OH; 20:1) to give probe **NIR-TS** as a dark purple solid (0.64 g, 53%). ^{1}H NMR (600 MHz, CDCl3) δ 13.30 (s, 1H), 8.54 (s, 1H), 8.30 (s, 1H), 8.05 (d, J = 9.4 Hz, 1H), 8.00 (d, J = 8.1 Hz, 1H), 7.97 (d, J = 8.0 Hz, 1H), 7.58 – 7.54 (m, 2H), 7.48 (t, J = 7.6 Hz, 1H), 7.31 (d, J = 8.7 Hz, 2H), 6.87 (s, 1H), 3.71 (d, J = 7.0 Hz, 4H), 3.04 (s, 2H), 2.98 (s, 2H), 1.99 (s, 2H), 1.40 (s, 6H), 1.27 (s, 3H). ^{13}C NMR (151 MHz, CDCl3) δ 168.76 (s), 162.59 (s), 159.13 (s), 156.33 (s), 154.74 (s), 151.48 (s), 149.76 (s), 133.97 (s), 133.20 (s), 132.55 (s), 131.85 (s), 130.12 (s), 128.78 (s), 128.51 (s), 126.89 (s), 125.87 (s), 124.11 (s), 123.77 (s), 122.08 (s), 121.62 (s), 119.81 (s), 118.35 (s), 116.73 (s), 94.98 (s), 46.33 (s), 29.62 (s), 27.43 (d, J = 9.7 Hz), 21.55 (s), 20.64 (s). HR-MS [probe]$^{+}$: m/z Calcd 507.2101, Found 507.2113(Figure S1).

Preparation of Solutions of Probe and Analytes. Stock solution of **NIR-TS** (2 mM) were prepared in DMSO. Stock solutions of 100 mM Cys, Hcy, 200 mM Na_2SO_3, GSH and other competing spieces were prepared by direct dissolution in deionized water. All chemicals used were of analytical grade.

General Fluorescence Spectra Measurements. All the detection experiments were measured in PBS (containing 5 percent ethanol, pH 7.4). The procedure was as follows: into a PBS system containing 10 μM **NIR-TS**, an analyte sample was added. The process was monitored by a fluorescence spectrometer.

Cell Culture and Imaging. The HeLa cells were grown in 1640 medium supplemented with 12% Fetal Bovine Serum and 1% antibiotics at 37 °C in a humidified environment of 5% CO_2. Cells were plated on a 6-well plate and allowed to adhere for 24 h. Before the experiments, cells were washed with PBS 3 times.

MTT Assays. The cytotoxicity of **NIR-TS** was tested by MTT. Hela cells were cultured in 96-well plates at a density of 4000 cells/well at 37°C in a 5% CO_2 incubator for 24 h. The cells were incubated with **NIR-TS** for 12 and 24 h, respectively. Then, 20 μL of MTT solution was added and the absorbance at 490 nm was examined.
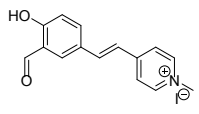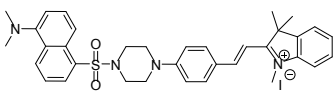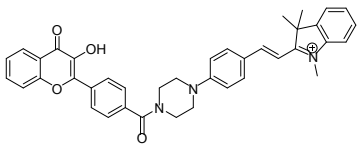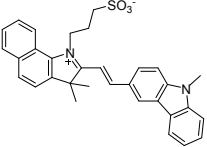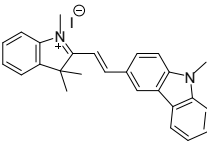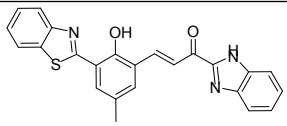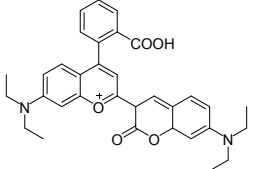
***In-vivo* imaging.** Both probe **NIR-TS** and analytes were subcutaneously injected in mice.
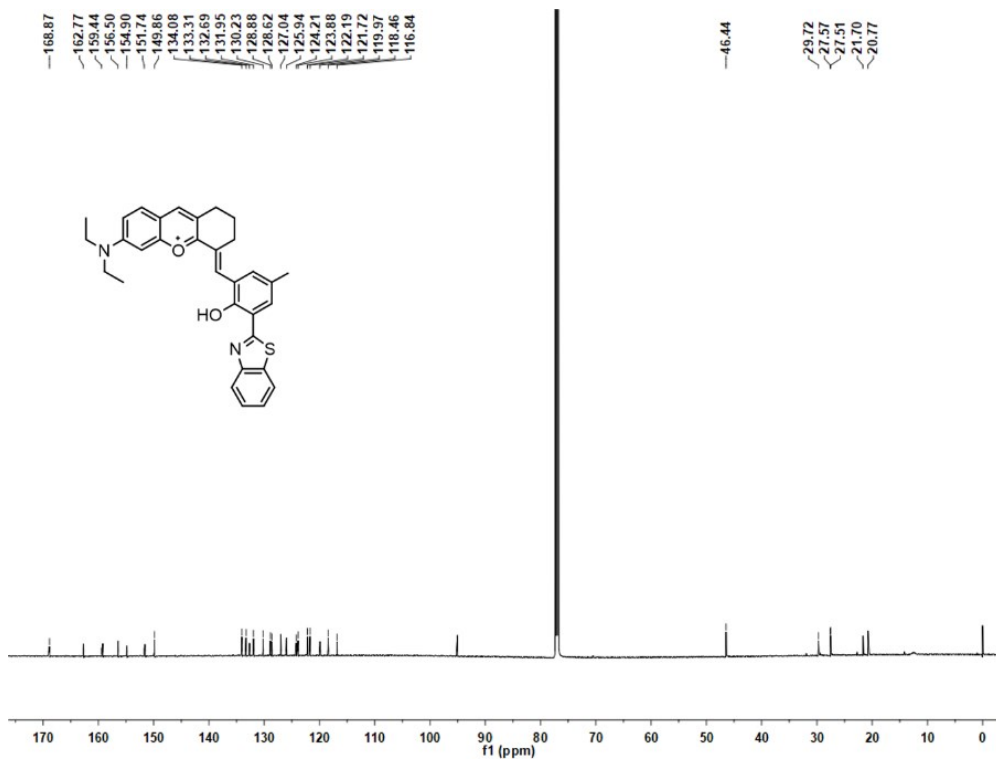
Computational methods.

The density functional theory (DFT) and time-dependent DFT (TD-DFT) calculations were carried out using Gaussian 16A.[1] All structure optimizations were performed without constraints using M06-2X functional and Def2SVP basis set.[2] Solvation effects in water were taken into account using the SMD model employing state-specific equilibrium solvation.[3] We also conducted frequency checks to ensure that stable molecular structures were obtained in both the ground and the excited states.

II: Figures

Table S1 The details of the reported probe for sulfite.

Probe	Ex(nm)	Em (nm)	Stokes shift (nm)	Solvent System	LOD (nM)
	460[6]	550	90	DMSO/PBS(9:1)	13.1
	410[7]	530; 582	172	DMF/PBS (3:7)	100
	345[8]	530; 590	245	DMF/PBS (1:3)	16
	405[9]	463; 625	220	PBS	58
	350[10]	490; 590	240	DMF/PBS (3:7)	150
	350[11]	542	192	DMSO:PBS(3:7)	22.7
	410[12]	480; 690	280	PBS	4.7
This work	**550**	**836**	**286**	**EtOH:PBS(5:95)**	**67**

Scheme S1: The **NIR-TS** synthesis compound **NIR-TS.**

*Compounds **1** and **2** were synthesized according to the references.

Figure S1: ^{1}H NMR (100 MHz) spectrum and ^{13}C NMR (100 MHz) spectrum of **NIR-TS** in CCl$_3$D and the HR-MS of **NIR-TS**.

168.87
162.77
159.44
156.50
154.90
151.74
149.86
134.08
133.31
132.69
131.95
130.23
128.88
128.62
127.04
125.94
124.21
123.88
122.19
121.72
119.97
118.46
116.84

46.44

29.72
27.57
27.51
21.70
20.77

170 160 150 140 130 120 110 100 90 80 70 60 50 40 30 20 10 0
f1 (ppm)

RHX0608-1 #8-15 RT: 0.10-0.17 AV: 4 NL: 9.13E7
T: FTMS + p ESI Full ms [150.0000-1000.0000]

507.21131

198.12801
229.14125
274.27439
318.30061
437.19414
482.24454
529.19273
545.16636
654.33221
760.35775
858.43053
934.37214

Relative Abundance

200 300 400 500 600 700 800 900 1000
m/z

Cald: 507.2101
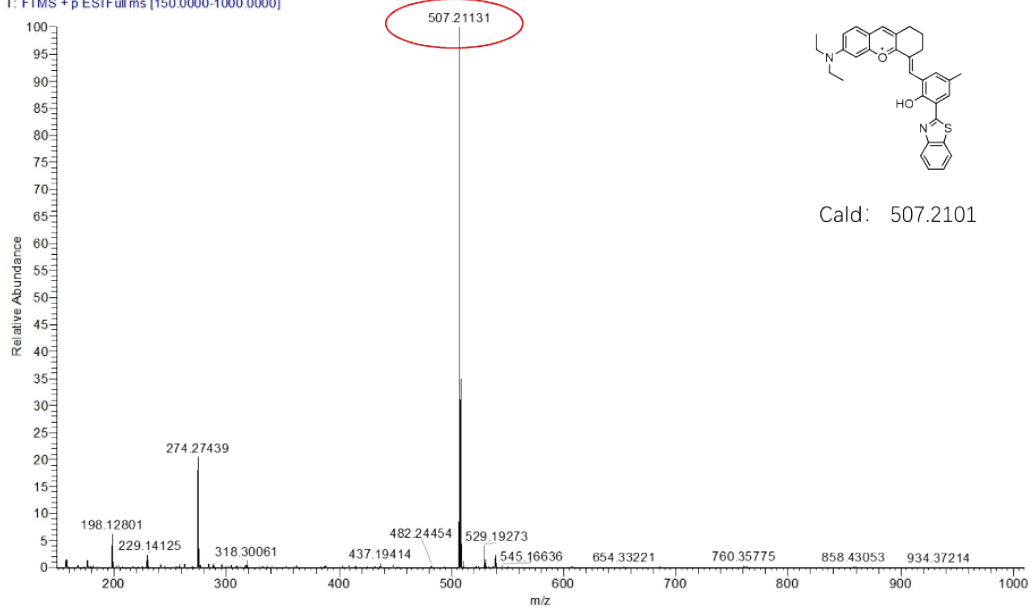
Figure S2: (A) UV-vis absorption spectra responses of **NIR-TS** (30 μM) toward different concentrations of Na_2SO_3; (B) Fluorescent responses of **NIR-TS** (10 μM) toward different concentrations of Na_2SO_3 in NIR region; (C) Working curve of **NIR-TS** for Na_2SO_3 detection quantificationally (All data was the average value obtained from three independent experiments); (D) Fluorescent intensity at 836 nm of probe itself and probe-Na_2SO_3 system at different pH levels. λ_{ex} = 550 nm; slit, 5 nm /10 nm.

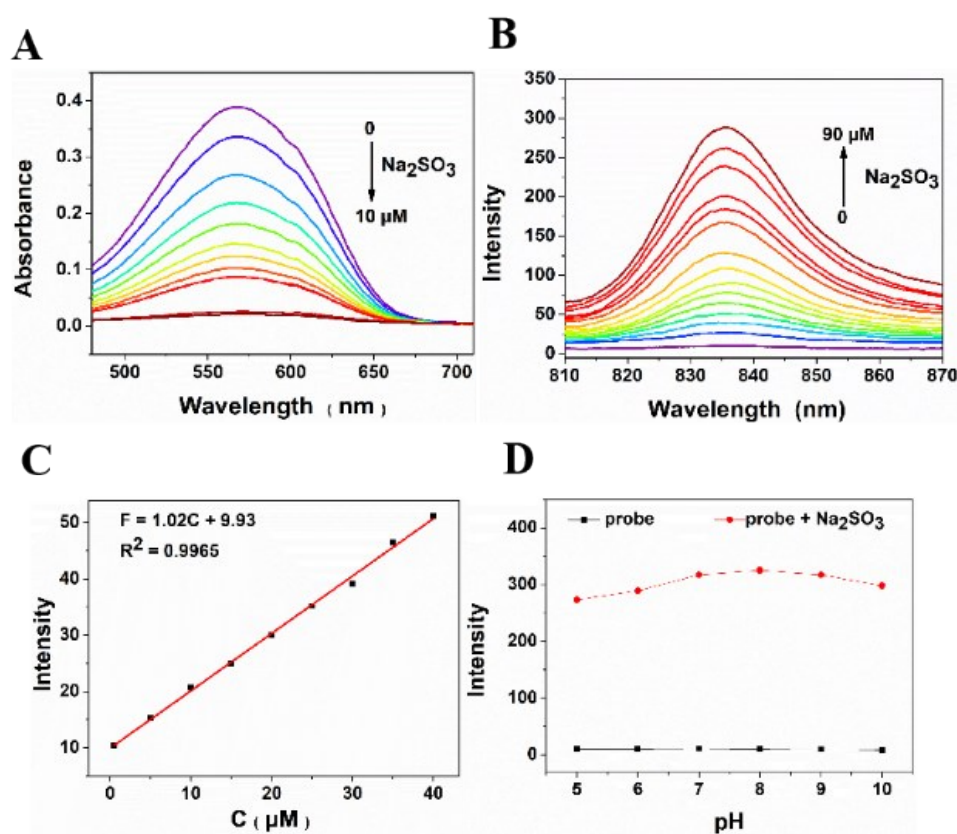**Figure S3:** Time-dependent fluorescence intensity at 836 nm of the probe (10 μM)
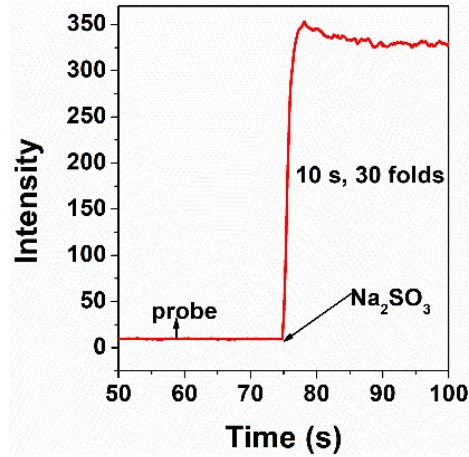
before and after adding 1mM Na_2SO_3

Figure S4: Intensities at 836 nm of probe **NIR-TS** (10 µM) upon addition of different analytes (1 mM).
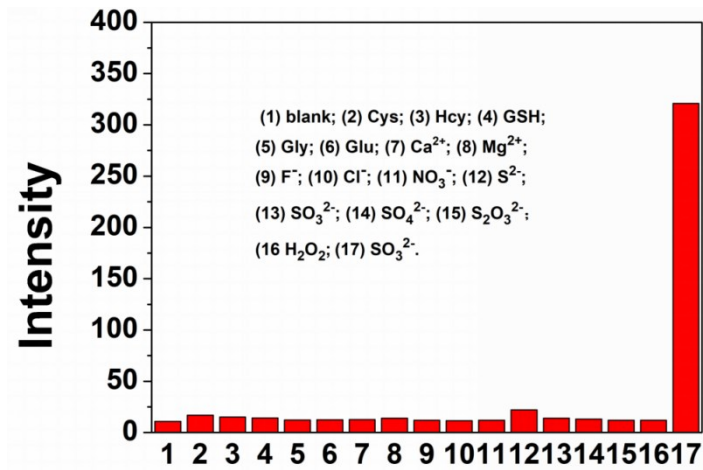

(1) blank; (2) Cys; (3) Hcy; (4) GSH;
(5) Gly; (6) Glu; (7) Ca^{2+}; (8) Mg^{2+};
(9) F^-; (10) Cl^-; (11) NO_3^-; (12) S^{2-};
(13) SO_3^{2-}; (14) SO_4^{2-}; (15) $S_2O_3^{2-}$;
(16 H_2O_2; (17) SO_3^{2-}.

Figure S5: The HR-MS of the **NIR-TS**-Na$_2$SO$_3$ system.

Figure S6: Schematic illustration of (a) **NIR-TS** during photoexcitation and photo-deexcitation processes and (c) the ESIPT process from **E** to **K** and the corresponding excitation/de-excitation energies and oscillator strength (*f*) in water. Optimized molecular structures and the corresponding electron and hole distributions of (b) **NIR-TS** and (d) **E** and **K** during photoexcitation and photo-deexcitation processes in water. The energy levels in (a) and (c) were not drawn to scale for clarity.
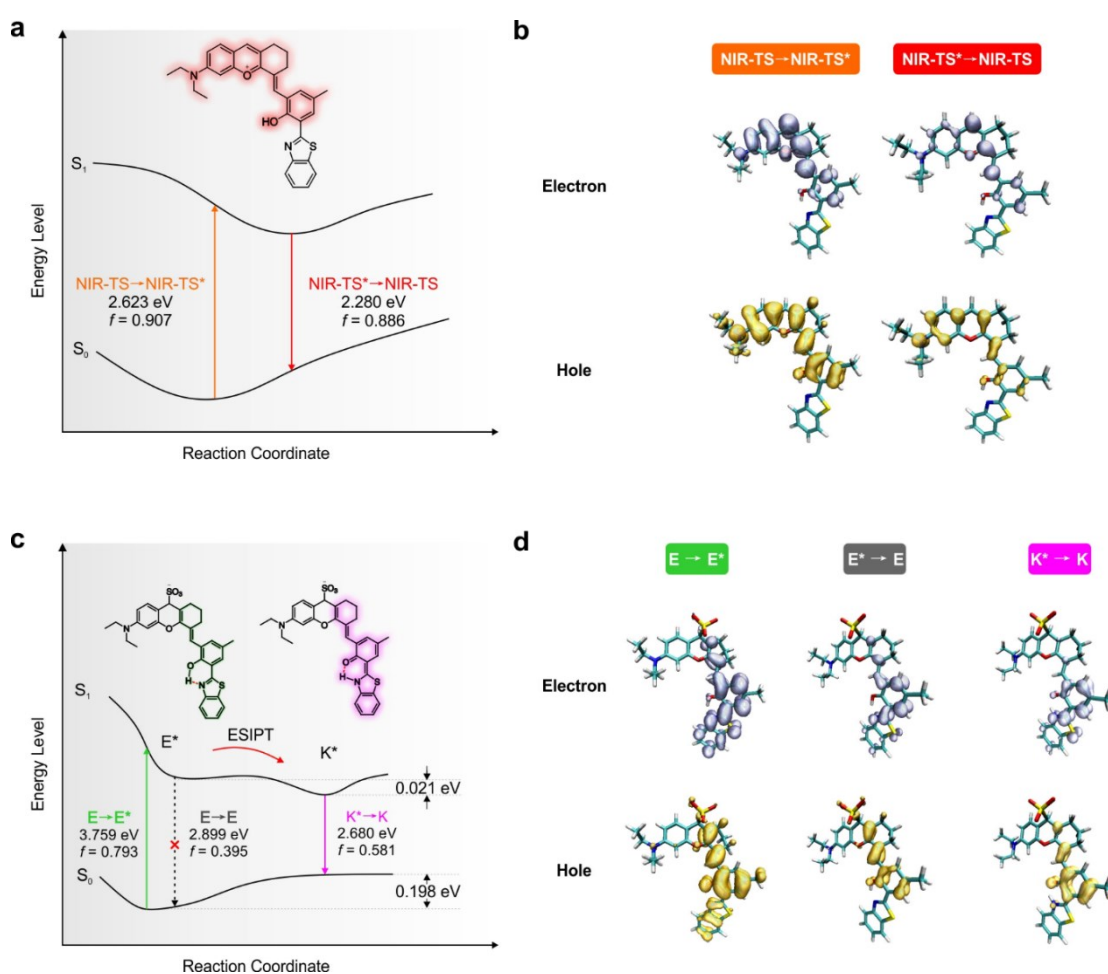
Figure S7: Cell viability estimated by MTT-8 assay with Hela cells, which were cultured in the presence of 0-50.0 μM **NIR-TS** for 12 h and 24 h.
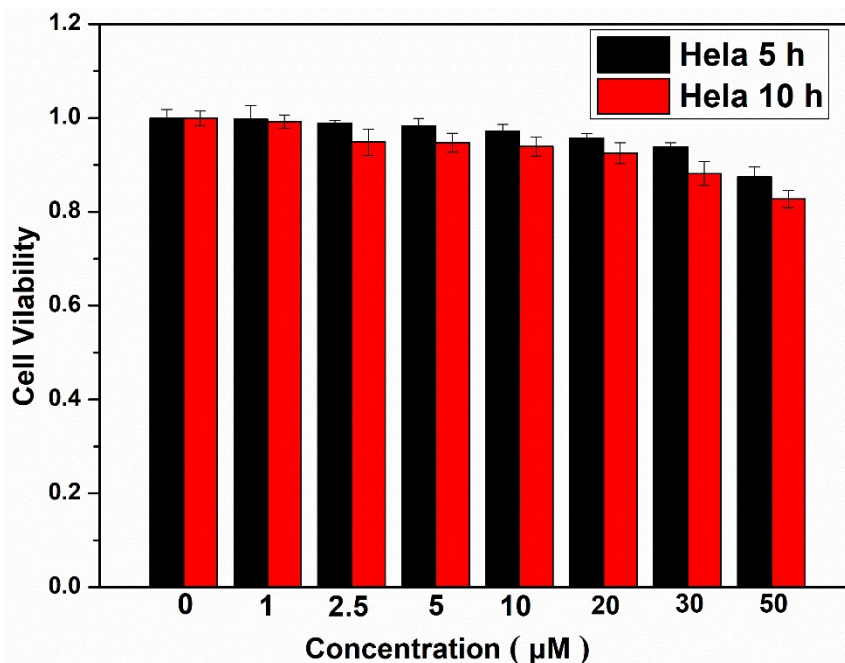

Figure S8: Co-staining of HeLa cells with **NIR-TS** (10 μM) for 10 min and MitoTracker green (0.5 μM) for 15 min successively. (a) Red channel (b) Green channel (c) Merge field (d) Bright field (e) Co-location results (f) Intensity for the both channels. Green channel: λex = 405 nm, λem = 480-520 nm; Red channel: λex = 561 nm, λem = 630−670 nm.
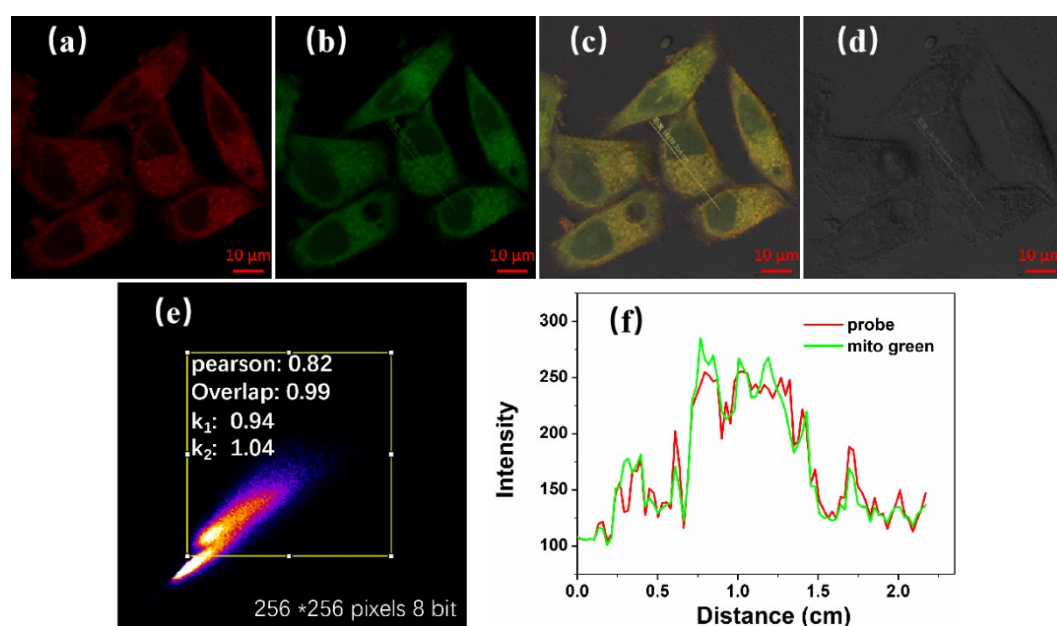
Figure S9: Concentration-dependent images of Hela cells incubated with probe **NIR-TS** and Na₂SO₃**(Left);** Intensity profiles of regions of interest (Right).
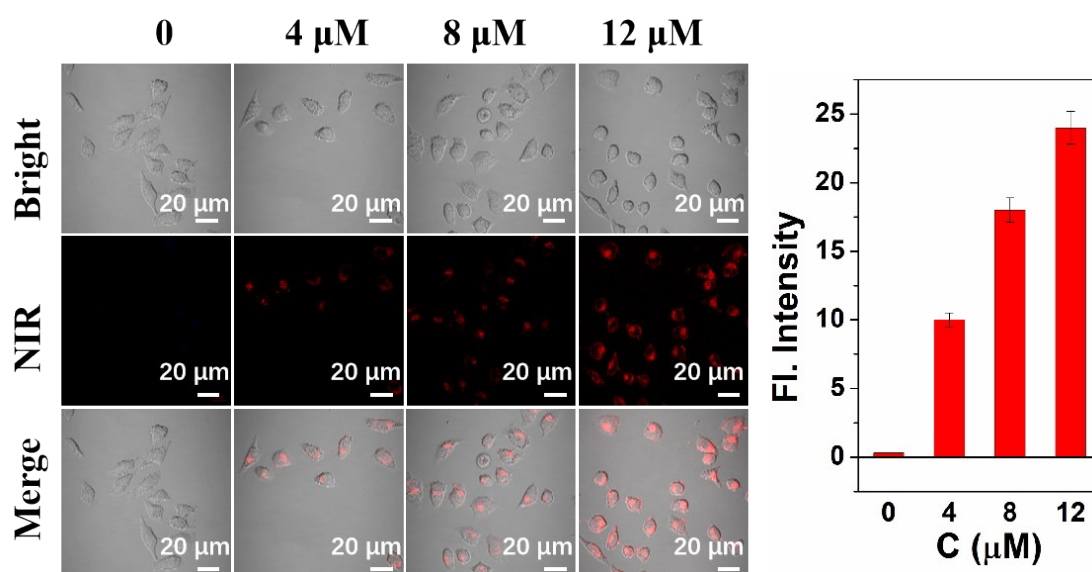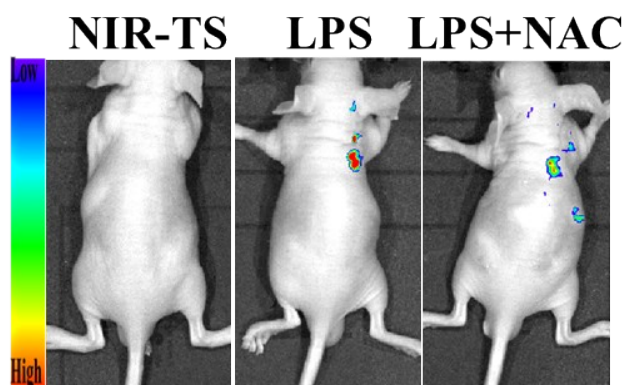

Figure S10: The NIR fluorescence images of mice incubated with **NIR-TS** (10 μM), **NIR-TS** (10 μM) with LPS, and **NIR-TS** with LPS and NAC (200 μM).

Ⅲ：**References**

[1] D. Dahal, L. McDonald, X. Bi, C. Abeywickrama, F. Gombedza, M. Konopka, S. Paruchuri and Y. Pang, *Chem. Commun.*, 2017, **53**, 3697-3700.

[2] W. Zhang, F. Huo, Y. Zhang and C. Yin, *J. Mater. Chem. B***, 2019,**7**, 1945-1950.

[3] M. J. Frisch, G. W. Trucks, H. B. Schlegel, G. E. Scuseria, M. A. Robb, J. R. Cheeseman, G. Scalmani, V. Barone, G. A. Petersson, H. Nakatsuji, X. Li, M. Caricato, A. V. Marenich, J. Bloino, B. G. Janesko, R. Gomperts, B. Mennucci, H. P. Hratchian, J. V. Ortiz, A. F. Izmaylov, J. L. Sonnenberg, Williams, F. Ding, F. Lipparini, F. Egidi, J. Goings, B. Peng, A. Petrone, T. Henderson, D. Ranasinghe, V. G. Zakrzewski, J. Gao, N. Rega, G. Zheng, W. Liang, M. Hada, M. Ehara, K. Toyota, R. Fukuda, J. Hasegawa, M. Ishida, T. Nakajima, Y. Honda, O. Kitao, H. Nakai, T. Vreven, K. Throssell, J. A. Montgomery Jr., J. E. Peralta, F. Ogliaro, M. J. Bearpark, J. J. Heyd, E. N. Brothers, K. N. Kudin, V. N. Staroverov, T. A. Keith, R. Kobayashi, J. Normand, K. Raghavachari, A. P. Rendell, J. C. Burant, S. S. Iyengar, J. Tomasi, M. Cossi, J. M. Millam, M. Klene, C. Adamo, R. Cammi, J. W. Ochterski, R. L. Martin, K. Morokuma, O. Farkas, J. B. Foresman and D. J. Fox, *Journal*, 2016.

[4] Y. Zhao and D. G. Truhlar, *Theor. Chem. Acc.*, 2008, **120**, 215-241.

[5] A. V. Marenich, C. J. Cramer and D. G. Truhlar, *J. Phys. Chem. B* 2009, **113**, 6378-6396.

[6] G .Chen, W. Zhou, C. Zhao, Y. Liu, T. Chen, Y. Li and B. Tang, *Anal. Chem.,*2018, **90**, 12442-12448.

[7] D. P. Li, Z. Y. Wang, X. J. Cao, J. Cui, X. Wang, H. Z. Cui, J. Y. Miao, B. X. Zhao, *Chem. Comm.,* 2016, **52**, 2760-2763.

[8] D. P. Li, Z. Y. Wang, H. Su, J. Y. Miao, B. X. Zhao, *Chem. Comm.,* 2017, **53**, 577-580.

[9] Y. Liu, K. Li, K.X. Xie, L. L. Li,K. K. Yu, X.Wang, and X.Q. Yu, *Chem. Comm.,* 2016, **52**, 3430-3433.

[10] Y. Liu, K. Li, M. Y. Wu, Y. H. Liu, Y. M. Xie and X. Q. Yu, *Chem. Comm.,* 2015, **51**, 10236-10239.

[11] H. Niu, Y. Zhang, J. Tang, X. Zhu, Y. Ye, and Y. Zhao, *Chem. Comm.,* 2020, **82**, 10236-10239.

[12] T. Li, C. Yin, J. Chao, W. Zhang and F. Huo, *Sens. Actu. B,* 2020, **305**, 127336.